IJCSE International Journal of Computer Sciences and Engineering Open Access
Research Paper Vol.-7, Issue-5, May 2019 E-ISSN: 2347-2693

Multimodal Image Fusion Technique MIFT-HDWRT for Improvement of Diagnosis Abilities

Manvi[1*], Ashish Oberoi[2]

[1]RIMT University, Mandi-Gobindgarh, Panjab, India
[2]RIMT University, Mandi-Gobindgarh, Punjab, India

DOI: https://doi.org/10.26438/ijcse/v7i5.386391 | Available online at: www.ijcseonline.org

Accepted: 13/May/2019, Published: 31/May/2019

***Abstract*:** Complementary information is provided in Medical images like PET, MRI, and CT. To make the correct diagnosis these images are fused and are providing additional information for clinical analysis. This paper proposes a new medical image fusion based on the combined effect of Discrete Wavelet Transfrom (DWT), and Discrete Ripplet Transform (DRT). The images are transformed at the start into multi-resolution image using 2-level DWT. The resultant images are transformed again using DRT. Applying the common and most fusion rule and inverse DRT, the united coefficients of the approximation image is obtained by applying inverse DWT to the united coefficients. The performance of the united image is evaluated using metrics like PSNR, Entropy, Standard Deviation, and Structural Similarity Index measure and it outperforms the opposite existing ways.

***Keywords**:* Medical image fusion; Discrete Wavelet Transform; Discrete Ripplet Transform; Multiscale geometric analysis;

I. INTRODUCTION

Image fusion is the process of combining information from two or more images of a scene into a single composite image. The fused image so obtained, contains more information. The fused image is suitable for visual perception and computer analysis. The uncertainly and redundancy is reduced in the output and the relevant information is maximized.

Image transformation is important as it affects the information extraction quality [1]. Many fusion methods over the past years have used different decomposition methods like laplacian pyramid, contrast, pyramid transform, discrete wavelet transform, etc. [2-4]. Recently, a theory called Multiscale Geometric Analysis has been developed. Many Multiscale Geometric Analysis tools were proposed, such as ridgelet, curvelet, contourlet, bandelet, ripplet etc. [5-9] which has higher directional sensitivity.

This paper proposes a new algorithm "MIFT-HDWRT" for medical image fusion. The fusion is based on the integration of discrete wavelet transform (DWT) and discrete ripplet transform (DRT). It uses average and maximum fusion rule. DWT provide directional information in decomposition levels and contain unique information at different resolutions [10]. DRT is a higher dimensional generalization of the curvelet transform. It is designed to represent images or 2-D signals at different scales and different directions [11]. The rest of this paper is organized as follows. Section 2 explains DWT and Section 3 explain DRT. Section 4 gives the new algorithm "MIFT-HDWRT". Simulation results are given in section 5. Section 6 concludes the paper.

II. DISCRETE WAVELET TRANSFORM

The original concept and theory of wavelet-based multi-resoultion analysis came from Mallat [12]. Discrete Wavelet Transform (DWT) represents image variations at different scales. A wavelet is an oscillation and attenuated function and its integrals equal to zero. The wavelet transform is a mathematical tool which detects local features in a signal process. It can also be used to decompose two-dimensional (2-D) signals or images into different resolution levels for multi-resolution analysis. Wavelet transform is applied in many areas, such as texture analysis, data compression, feature detection and image fusion.

The DWT is a spatial-spectral decomposition that provides a flexible multi-resolution analysis of an image [13]. In a 2-D DWT, a 1-D DWT is first performed on the rows and then columns of the data by separately filtering and down sampling. This results in one set of approximation coefficients *LL* and three sets of detail coefficients *LH*, *HL*, *HH* representing the vertical, horizontal, and diagonal directions of the image as shown in Fig. 1 (a). The 2-D structures of the wavelet transform with two decomposition levels is shown in Fig. 1 (b).

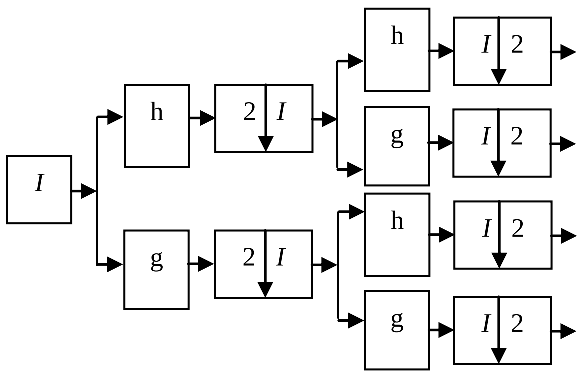

Fig. 1 (a) A structure of the DWT

<table>
<tr><td>LL2</td><td>HL2</td><td rowspan="2">HL</td></tr>
<tr><td>LH2</td><td>HH2</td></tr>
<tr><td colspan="2">LH</td><td>HH</td></tr>
</table>

Fig. 1 (b) 2-D DWT structure with labeled sub-bands in two-level decomposition

By recursively applying the same scheme to the *LL* sub-band a multi-resolution decomposition with a desired level can then be achieved. Therefore, a DWT with *K* decomposition, there is only one low frequency band (LL^K) as given in Fig. 1 (b) and the rest of bands are high frequency bands in a given decomposition level.

III. DISCRETE RIPPLET TRANSFORM

The ripplet transform overcomes the disadvantage of the wavelet transform. It represents edges in the images more efficiently. The images are represented at different scales and different directions. The curvelet transform can be obtained from DRT provided support is given as 1 and degree as 2. The scale parameter a, is sampled at dyadic intervals. The position parameter b and rotation parameters θ are sampled at equally spaced intervals. The scale, position and rotation parameters are in discrete form such that

$$a_j = 2^{-j}, \overrightarrow{b_k} = [c \cdot 2^{-j} \cdot k_1, 2^{-j/d} \cdot k_2]^T$$

and

$$\theta_l = {}^{2\pi}/_{c} \cdot 2^{-\lfloor j(1-{}^{1}/_{d}) \rfloor} \cdot l$$

where

$$\vec{k} = [k_1; k_2]^T, [.]^T$$

denotes the transpose of a vector and j, k_1, k_2, $l \in Z$. The degree of ripplets can take value from R. Since any real number can be approximated by rational numbers, d can be represented as d = n/m, n, m $\neq$ 0 $\in$ Z. In the frequency domain, the corresponding frequency response of ripplet function is in the form

$$\overline{p_j}(r,\omega) = {}^{1}/_{\sqrt{c}}\, a \frac{m+n}{2n} W(2^{-j} \cdot r) V({}^{1}/_{c} \cdot 2^{-\left\lfloor j\frac{m-n}{n} \right\rfloor} \cdot \omega - l)$$

Where *W* and *V* satisfy admissibility conditions as below

$$\sum_{j=0}^{+\infty} \left| W(2^{-j} r.) \right|^2 = 1$$

$$\sum_{l=-\infty}^{+\infty} \left| V(\frac{1}{c} \cdot 2^{-\lfloor j(1-{}^{1}/_{d}) \rfloor} \cdot \omega - l) \right|^2$$

The 'wedge' corresponding to the ripplet function in the frequency domain is

$$H_{j,l}(r,\theta) = \left\{ 2^{2j} \leq |r| \leq 2^{2j}, \left| \theta - \frac{\pi}{c} \cdot 2^{-\lfloor j(1-\frac{1}{d}) \rfloor}. l \right| \leq \frac{\pi}{2} 2^{-j} \right\}$$

The number of directions in the high-frequency region is controlled by the support *c*. The degree *d* controls how the number of directions changes across bands. For fixed *c*, the resolution in directions at each high-pass band is controlled by degree *d*. The number of directions at all high-pass bands is controlled by *c*, provided *d* is given. The final number of direction at each band is determined by the support *c* and degree *d*.

The discrete ripplet transform of an $M \times N$ image $f(n_1, n_2)$ will be in the form of

$$R_{j,\vec{k},l} = \sum_{n_1=0}^{M-1} \sum_{n_2=0}^{N-1} f(n_1,n_2) \overline{\rho_{j,\vec{k}.l}(n_1,n_2)}$$

The image can be reconstructed through inverse discrete ripplet transform

$$\tilde{f}(n_1, n_2) = \sum_j \sum_{\vec{k}} \sum_l R_{j,\vec{k},l}\, \rho_{j,\vec{k},l}\,(n_1, n_2)$$

IV. MIFT-HDWRT ALGORITHM

The new algorithm MIFT-HDWRT image fusion is given below:

- **Step 1:** Read the set of multimodal images (i.e. two images of different modality of same size).
- **Step II:** Perform single-level wavelet decomposition on both images to get approximation information (LL), horizontal details (HL), vertical details (LH), and diagonal details (HH) of the image.
- **Step III:** Perform single-level wavelet decomposition on approximation information (LL) of to get second-level approximation information (LL2), horizontal details (HL2), vertical details (LH2), and diagonal details (HH2).
- **Step IV:** Apply Ripplet transform on the detailed component of the image and the image result would be ripplet transform applied on all the detailed component of the image.
- **Step V:** Calculate the average values of horizontal details (HL2), and diagonal details (HH2) from both decomposed images respectively with the decomposition as well as after applying the transformation on detailed components.

  F(x, y) = (A(x, y) + B(x, y)) / 2

  Where, A (x, y), B (x, y) will be the input image, F (x, y) will be the fused image, and point (x,y) will be the pixel value.
- **Step VI:** Choose the maximum values of approximation information (LL2), and vertical details (LH2) by comparing the coefficient of both decomposed images respectively.

  F(x,y)= Max(A(x , y)+ B(x , y))
- **Step VII:** Reconstruct the approximation image (LL) by inverse wavelet transform using second-level approximation information (LL2), horizontal details (HL2), vertical details (LH2), and diagonal details (HH2).
- **Step VIII:** Apply the fusion rule on details of first-level decomposition as follows:

  i. Calculate the average values of horizontal details (HL), and diagonal details (HH) from both decomposed images respectively.

  ii. Choose the maximum values of vertical details (LH) by comparing the coefficient of both decomposed images.
- **Step IX:** Reconstruct the image by inverse wavelet transform on the Ripplet transformed image using wavelet transform.
- **Step X:** Apply Histogram Equalization.

4.1 Fusion Rule for the approximation and vertical coefficients.

Calculate the approximation and vertical details of the wavelet transform of image 1 as *LL1* and that of image 2 as *LL2*. Decompose *LL1* and *LL2* further using DWT. Let the ripplet coefficients be represented as X_L and Y_L. The ripplet coefficients are applied to 2nd level decomposed image *LL2, LH2*. The ripplet coefficients are then fused using maximum fusion rule (*F*) as given below

F(x,y)= Max(A(x , y)+ B(x , y))

Inverse DRT is applied to F and the low frequency fused coefficients are obtained.

4.2 Fusion rule for the horizontal and diagonal coefficients.

Calculate the approximation and vertical details of the wavelet transform of image 1 as *LL1* and that of image 2 as *LL2*. Decompose *LL1* and *LL2* further using DWT. Let the ripplet coefficients be represented as X_L and $Y_{L.}$ The ripplet coefficients are applied to 2nd level decomposed image *HL2, HH2*. The ripplet coefficients are then fused using average fusion rule (*F*) as given below

F(x, y) = (A(x, y) + B(x, y)) / 2

Inverse DRT is applied to F and the high frequency fused coefficients are obtained.

V. SIMULATION RESULTS

The medical images used for the fusion are CT, MRI, and PET images. The combination used for fusion is MRI with PET, and CT with PET is shown in Fig. 3(a), Fig. 3(b) and Fig. 4(a), Fig. 4(b) respectively.

The wavelet used for the fusion is daubechies walvelet, 'db6'. The DRT is performed with fixed support (c=1) and for degree d = 3.

The linking range is taken as 3×3 and the convolution kernel is given as:

$$W = \left[\left[\begin{matrix} \frac{1}{\sqrt{2}} & 1 & \frac{1}{\sqrt{2}} \\ 1 & 0 & 1 \\ \frac{1}{\sqrt{2}} & 1 & \frac{1}{\sqrt{2}} \end{matrix}\right]\right]$$

Simulation was carried out using MATLAB version 2016. The fused output obtained using MIFT-HDWRT and qualitative analysis is shown in Fig. 5 (a), (b) respectively.

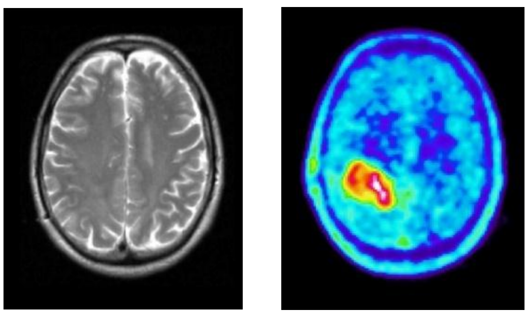

(a) (b)

Fig.3. input images (a) MRI image; (b) PET image

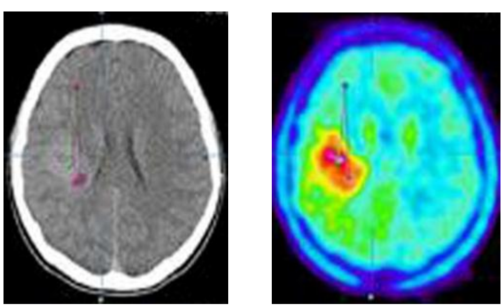

(a) (b)

Fig.4. input images (a) CT image; (b) PET image

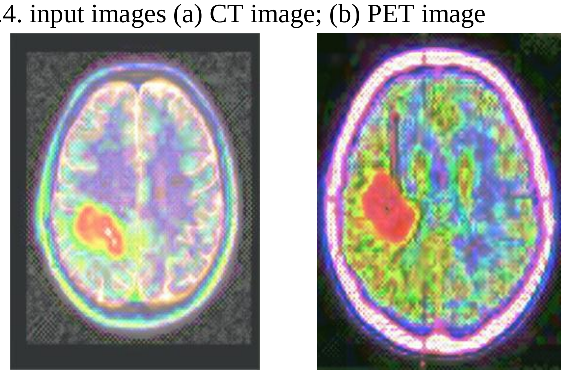

(a) (b)

Fig.5. fused output (a) MRI with PET; (b) CT with PET

Qualitative analysis is used for the subjective evaluation of the images. As subjective evaluation differs based on visual acuity, quantitative analysis is necessary for analyzing the quality of the fused image. Different parameters like PSNR, Entropy, Standard Deviation (SD) and Structural Similarity Index Measure (SSIM) are evaluated on 35 sets of images and compared with the existing methods for proving the effectiveness of the MIFT-HDWRT technique. Table 1 shows the value of quality measures implemented on MIFT-HDWRT, and Existing Method.

Table 1: Qualitative Analysis of MIFT-HDWRT and Existing Method

Input Image	Quality Factor	MIFT-HDWRT	Existing Method
MRI with PET	PSNR	10.7102	9.7359
	Entropy	7.3711	6.4068
	SD	66.3818	46.138
	SSIM	0.6386	0.2155
CT with PET	PSNR	13.8593	11.5741
	Entropy	7.9241	7.2406
	SD	50.4546	42.1099
	SSIM	0.423	0.2127

The quality metrics PSNR, Entropy, SD, and SSIM are shown graphically in Fig. 6, and Fig. 7 for comparison based on Table 1 respectively.

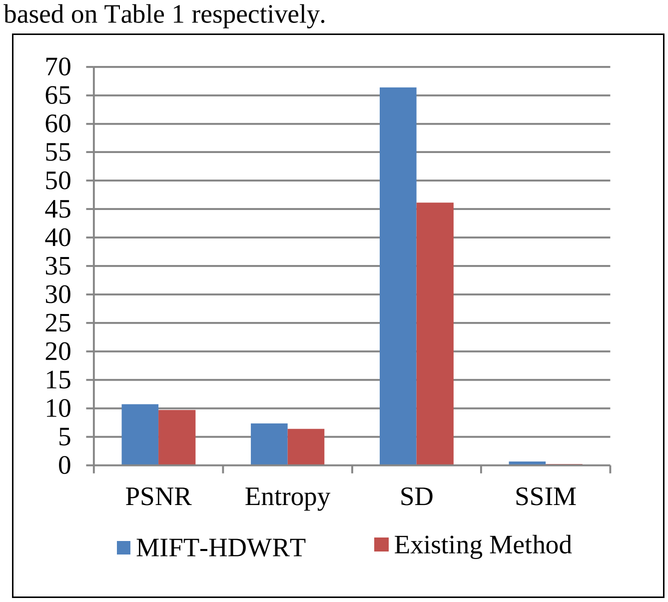

Fig.6. Qualitative Analysis of MRI with PET fusion.

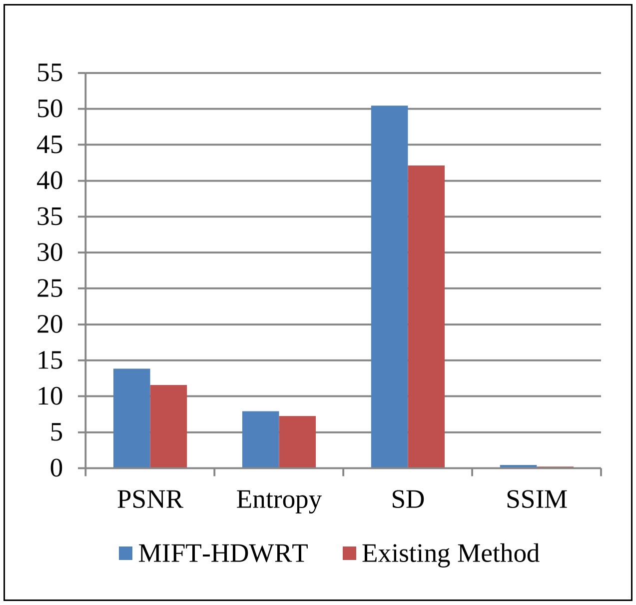

Fig.7. Qualitative Analysis of CT with PET fusion.

VI. CONCLUSION

In this paper, medical image fusion has been performed using the combined effect of DWT and DRT. The wavelet transform is a mathematical tool that can detect local features. DRT has better advantage of directionality and localization. The maximum fusion rule is applied to fuse the approximation, and vertical details of the image. The detail images are fused using average fusion rule. The edges are defined clearly in the fused output of the MIFT-HDWRT. The entropy gives the information content of the image. The PSNR, Entropy, SD, SSIM of the MIFT-HDWRT is high compared to the existing method. The standard deviation which is the square root of the variance reflects the information spread in the data. The MIFT-HDWRT has good clarity compared to the existing methods. The quantitative analysis clearly indicates that the MIFT-HDWRT outperforms other existing methods.

REFERENCES

[1] Agarwal, J., and Bedi, S.S. (2015), "*Implementation of hybrid image fusion technique for feature enhancement in medical diagnosis*", Springer Open Journal – Human-centric Computing and Information Sciences, Vol. 5, No. 3, pp. 1-17.

[2] Bedi, S.S., Agarwal, J., and Agarwal, P. (2013), "*Image Fusion Techniques and Quality Assessment Parameters for Clinical Diagnosis: A Review*", International Journal of Advanced Research in Computer and Communication Engineering, Vol. 2, No. 2, pp. 1153-1157.

[3] Bhanusree, C., and Chowdary, A.R. (2013), "*A Novel Approach of image fusion MRI and CT image using Wavelet family*", International Journal of Application or Innovation in Engineering & Management, Vol. 2, No. 8, pp. 1-4.

[4] Bhavana, V., and Krishnappa, H.K. (2016), "*Fusion of MRI and PET Images using DWT and Adaptive Histogram Equalization*", IEEE – International Conference on Communication and Signal Processing, Vol. 10, No. 9, pp. 0795-0798.

[5] Cheng S., He, J., and Lv, Z. (2008), "*Medical Image of PET/CT Weighted Fusion Based on Wavelet Transform*", International Conference on Bioinformatics and Biomedical Engineering, Vol. 8, No. 3, pp. 2523-2525.

[6] Chiorean, L., and Vaida, M.F. (2009), "*Medical Image Fusion Based on Discrete Wavelet Transform Using Java Technology*", IEEE conference on Information Technology, Vol. 31, No. 8, pp. 55-60.

[7] Do, M.N., and Vetterli, M. (2005), "*The contourlet transform: an efficient directional multiresolution image representation*", IEEE Transactions on image processing, Vol. 14, No. 12, pp. 2091-2106.

[8] Emmanuel, C., Laurent, D., David, D., and Lexing, Y. (2005), "*Fast discrete curvelet transforms based on Multiscale Model*", IEEE Transactions on image processing, Vol. 5, No. 2, pp. 861-899.

[9] Flusser, J., Sroubek, F., and Zitova, B. (2007), "*Image Fusion: Principles, Methods, and Applications*", Tutorial EUSIPCO, pp. 7-22.

[10] Indira, K.P., Hemamalini, R.R., and Indhumathi, R. (2015), "*Pixel based Medical Image Fusion Techniques using Discrete Wavelet Transform and Stationary Wavelet Transform*", Indian Journal of Science and Technology, Vol. 8, No. 26, pp. 1-7.

[11] James, A.P., and Dasarathy, B.V. (2014), "*Medical image fusion: A survey of the state of the art*", Elsevier Information Fusion, Vol. 19, No. 14, pp. 4-19.

[12] Mallat, C., Lan, T., Xiao, Z., Li, Y., Ding, Y., and Qin, Z. (2014), "*Multimodal Medical Image Fusion Using Wavelet Transform and Human Vision System*", IEEE Transaction, Vol.9, No. 14, pp. 491-495.

[13] Mukane, S.M., Ghodake, Y.S., and Khandagle, P.S. (2013), "*Image enhancement using fusion by wavelet transform and laplacian pyramid*", International Journal of Computer Science Issues, Vol. 10, No. 2, pp. 122-126.

[14] Oberoi, A., and Singh, M. (2012), "*Content Based Image Retrieval System for Medical Databases (CBIR-MD) – Lucratively tested on Endoscopy, Dental and Skull Images*", IJCSI International Journal of Computer Science, Vol. 9, No. 1, pp. 300-306.

[15] Patel, J.M., and Parisk, M.C. (2016), "*Medical Image Fusion Based on Multi-Scaling (DRT) and Multi-Resolution (DWT) Techniques*", IEEE – International Conference on Communication and Signal Processing, Vol. 10, No. 9, pp. 0654-0657.

[16] Piella, G. (2003), "*A general framework for multiresoultion image fusion: from pixels to regions*", Information Fusion, Vol. 4, No. 3, pp. 259-280.

[17] Qi-guang, M., Cheng, S., Peng-fei, X., Mei, Y., and Yao, S. (2011), "*A novel algorithm of image fusion using shearlets*", J Optics Communication, Vol. 284, No. 5, pp. 1540-1547.

[18] Sharmila, K., Rajkumar, S., and Vijayaranjan, V. (2013), "*Hybrid method for Multimodality Medical image fusion using Discrete Wavelet Transform and Entropy concepts with Quantitative Analysis*", IEEE – International conference on Communication and Signal Processing, Vol. 9, No. 13, pp. 489-493.

[19] Susmitha, V., and Pancham, S. (2009), "*A novel architecture for wavelet based image fusion*", World Academy of Science Engineering and Technology, Vol. 57, No. 7, pp. 372-377.

[20] Toet, A., Van, R.J., and Valeton, J.M. (1989), "*Marging thermal and visual images by a contrast pyramid*", Optical Engineering, Vol. 28, No. 7, pp. 789-792.
[21] Umaamaheshvari, A., and Thanushkodi, K. (2010), "*Image Fusion Techniques*", International Journal of Research and Reviews in Applied Sciences, Vol. 4, No. 1, pp. 69-74.
[22] Xu, J., Yang, L., and Wu, D. (2010), "*Ripplet: A new transform for image processing*", Elsevier Journal of Visual Communication & Image Representation, Vol. 21, No. 10, pp. 627-639.

